

LAYER-BY-LAYER NANOSCALE BONDLINES FOR MACROSCALE ADHESION

Yu Zhou,^a Scott Rennecker,^{a*} Karthik V. Pillai,^a Qingqing Li,^a Zhiyuan Lin,^a and W. Travis Church^a

The objective of this study was to test the bonding performance of nanoscale bondlines, which were fabricated with polyelectrolytes by layer-by-layer assembly process onto wooden substrates. In this study, environmental scanning electron microscopy (ESEM) was used to characterize adsorbed multilayers of polyacrylic acid and polyallylamine hydrochloride on the wood surface. Cross-linking between PAA and PAH layers at various temperatures was studied using Fourier Transform Infrared Spectroscopy (FTIR). The evaluation of polyelectrolyte multilayers as bonding agents for wood was conducted through compression shear block and flexural bending tests. Altogether, this research demonstrates a route to utilize nanoscale coatings as bonding agents.

Keywords: Adhesion; Composites; Layer-by-layer films; Multi-layer films; Polyelectrolytes

Contact information: a: Department of Wood Science and Forest Products, Virginia Tech, 230 Cheatham Hall, Blacksburg, VA 24061USA; *Corresponding author: srenneck@vt.edu

INTRODUCTION

Biological hierarchical structures have suitable levels of adhesion at each distinct level of organization from the molecular to macroscale arising from the highly functional chemistry associated with their protein or polysaccharide based structures (Baer et al. 1992). Typically, there are no adhesive bondlines that have dimensions in the range of 10^{-3} to 10^{-5} m. As a prototypical example, nacre has only 10's of nanometers of adhesive between every layer of aragonite tiles (Wang et al. 2001), and at the upper extreme, intercellular layers within plants only reach a few hundred nanometers. By contrast, synthetic composite material bondlines are usually on the order of micrometers and greater, creating the adhesive as its own phase. Adhesive systems for these materials are often fabricated based on the chemistry of the substrates and create a distinct interface on the scale of microns. Adhesives can make up 2 to 10% by weight in particulate and laminate composites to more than half of the material in fiber reinforced thermoplastic composites. Reducing adhesive consumption and combining dissimilar materials with a single adhesive system are challenging issues that have potential to yield increased composite performance and reduced costs if synthetic analogs to the bioinspired structures are achieved.

Nanoscale surface coatings have been fabricated on many substrates using layer-by-layer (LbL) assembly of polyelectrolytes. LbL assembly occurs in liquid medium, where oppositely charged polymers are assembled in single digit nanometer layers by sequential exposure, reversing the surface charge with each adsorbing layer of

polyelectrolyte (Decher 1997). Modification of both organic and inorganic substrates can occur with priming materials such as branched polyethylenimine (PEI) (Kolasinska et al. 2007). Furthermore, chemical derivitization of PEI with catechol provides a mussel-inspired universal priming layer for low surface energy materials such as poly(tetrafluoroethylene) and polyethylene (Lee et al. 2008). Deposition of layers does not have to occur by submersion; spraying applications (Izquierdo et al. 2005, Schlenoff et al. 2000), which are easily automated (Krogman et al. 2007) have shown decreased fabrication times by 25 fold. These developments in processing can help realize the potential these unique LbL films have to offer for industrially manufactured materials. While nanoscale LbL films were used to create novel coatings on surfaces such that are antireflective (Cebeci et al. 2006), superhydrophobic (Han et al. 2005, Li et al. 2009), and corrosion inhibitors (Kachurina et al. 2004, Shchukin et al. 2006), they also have demonstrated the ability to bond smooth substrates together (Matsukuma et al. 2009) or enhance adhesion in paper (Lingstrom et al. 2006, Lvov et al. 2006, Notley et al. 2005, Wågberg et al. 2002).

Recently, we reported on the process of forming layered films on wood substrates, relating how the deposition of the initial polyelectrolyte layer was influenced by pH and electrolyte concentration of the treating solution (Renneckar and Zhou 2009). While wood surfaces are heterogeneous in structure, roughness, and chemistry, optimized conditions were reported to link these polyelectrolyte films to wood substrates. To form layered films on wood, PEI was deposited under alkaline pH in the absence of added electrolyte, followed by sequential adsorption of two weak polyelectrolytes, polyacrylic acid (PAA) and polyallylamine hydrochloride (PAH). Based on the pH of the solution, each bi-layer was estimated to be 9 nm in thickness (Choi and Rubner 2005), with a linear increase in polyelectrolyte on the wood substrate as function of the number of dip cycles (Renneckar and Zhou 2009).

In this paper we report an adhesive system for both macroscale and microscale objects with heterogeneous chemistry and roughness through the creation of highly controlled thin films on substrates using LbL assembly. Specifically we provide an example of bonding solid wood and wood fibers with thermally crosslinkable polyelectrolyte layers of PAA and PAH. These bondlines are miniaturized, similar in dimension to adhesive interfaces found in nature, and thinner than the inherent roughness of the substrates.

EXPERIMENTAL

Materials

Polyacrylic acid (PAA, $M_w=100,000$), polyallylamine hydrochloride (PAH, $M_w=70,000$), and polyethylenimine (PEI, $M_w=25,000$) were obtained from Sigma Aldrich. All solutions were prepared using ultra-pure water (Milli-Q plus system, Millipore) with a resistivity of 18.2 M Ω .cm. Wood specimens were cut from mature sapwood of southern yellow pine (*Pinus spp.*) or were obtained from a pressurized disc refiner (further information about the fiber refining pressure is not available).

Methods

LbL formation on wood blocks

Pinus spp. (southern yellow pine) was cut into 20 blocks (32cm x 6.5cm x 2cm) with grain direction parallel to the longest dimension and subsequently saturated with water. Aqueous solutions of 1.0 mg/mL PEI, 0.6 mg/mL PAA, and 0.27 mg/mL PAH were freshly prepared and adjusted to pH 10.5, 5.0, and 5.0 respectively. Samples were first treated with a solution of PEI, and then subsequently treated with PAA and PAH. The wood was moved manually from 2 L containers, allowing 30 min deposition time per layer and rinsed with ultrapure water for 30 min between each layer. After coating each wood substrate, the strips were placed in a conditioning chamber with a relative humidity of $50\pm 2\%$ and a temperature of $23\pm 1^\circ\text{C}$ for a period of 7 days. The purpose of this step was to slowly reduce the moisture content of the wood so there was no surface checking of the blocks during drying. Commercial phenol formaldehyde (PF) adhesive (Dynea North America, OSB core resin, 50% solids) was coated onto similar sized wood blocks as a control.

LbL formation on wood fibers

The LbL coating process was repeated with pressurized refined wood fiber. The fibers were first saturated with water for 24 hours at a 5% w/v consistency. Subsequently, the fibers were isolated using a centrifuge at 4000 RPM in one liter centrifuge containers. Fibers were sequentially exposed to the polyelectrolytes as listed above with the same treating time. The fibers were split into two batches after PEI(PAA/PAH)₃ treatment and one batch received one additional polyelectrolyte treatment, so 50% of the fibers had a terminal PAA coating while 50% of the fibers had a PAH coating.

Composite formation and specimen testing

For each coating type, PEI(PAA/PAH)_n, two coated wood strips were wetted with water and placed into the hotpress preheated to 180°C . The terminal surface layer of each block was opposite in nature (i.e. PAA on one block and PAH on the other face). The samples were pressed for 30 minutes with a maximum pressure of 2.1 MPa (the bondline temperature reached 150°C for the last ten minutes of pressing). After hot pressing, bonded specimens were kept in the conditioning chamber for 7 days and machined into compression shear block specimens following ASTM-D905 guidelines with the noted exception that the substrate thickness was half of the prescribed thickness. This change was implemented to increase the speed of heat flow to the bondline.

The fiber with opposite terminal surface charges was mixed together in a container at an approximate 2% consistency and poured into a TAPPI handsheet sheet apparatus (159 mm diameter). The handsheet apparatus provided a method to create a fibrous cake that could be transferred into a steel mold. Samples were transferred from the handsheet screen, moist, into a steel mold 151x 151mm and compression molded following the above mentioned press cycle. The test plaques were then cut into 12 mm wide strips for flexural testing.

Mechanical evaluation of samples

Half of the 28 shear blocks for each joint type were randomly chosen for mechanical testing in their dry state. The other 14 shear blocks for each joint type were then prepared for a weathering test. First, all specimens were boiled in water for 4 hours. After drying for 20 hours in a conditioning chamber, they were boiled again for a period of 4 hours and then cooled in water at room temperature. The shear tests were then carried out on the wet samples. All specimens were tested in a United Testing System apparatus and subjected to a compression load following the ASTM-D 905 standard. The loading speed of the machine during the experiment was set to 0.51 mm/min. The load at the moment of failure was recorded by the acquisition system and calculated into the shear strength. After failure the wood samples were qualitatively evaluated for their amount of wood failure following ASTM-D 5266.

Fiber composite samples were cut for flexural tests were 63*12.7*3.18 mm with the span-to-depth ratio of 16:1. The three point bending tests were performed at a constant crosshead (midspan deflection) speed of 0.64 mm/min. The midspan deflection was determined by a linear variable differential transformer (LVDT) under the specimen in contact with it at the center of the support span.

Analytical characterization of thin films

FTIR experiments were performed on LbL films assembled on acid Piranha cleaned silicon wafers. An automated dipping robot was used to assemble the 15 bi-layers on each silicon wafer. Afterwards the samples were heated in a convection oven at the indicated temperatures. Silicon is transparent to infrared radiation; the samples were tested in transmission mode (Thermo Nicolet 8700) with 128 scans and a resolution of 8 cm^{-1} . SEM (FEI Helios 600 Nanolab) images of wood samples with 3 and 9 bi-layers were recorded after the samples were sputter coated with Au/Pd layer to reduce charging of the sample.

RESULTS AND DISCUSSION

Bonding of Wood Substrates with LbL Films

Substrates of solid wood with prepared LbL films were either, a) placed into contact under pressure (2.1 MPa) and heated (100°C at core) for 30 min, in order to deplete the water, similar to latex adhesives, or b) dried independently, rehydrated by spraying with water, and then heated and pressed under the same condition as described above. Once dried, the wooden substrates remain adhered together (Fig. 1). However, upon exposure to water, dimensional changes within the substrate combined with the hydrated LbL film caused immediate failure of the bonded specimen. While dimensional changes of wood can generate great pressure, the intermolecular forces within the LbL film are influenced by the dielectric constant of the medium surrounding the film (Israelachvili 1991). Hence, as the film becomes hydrated, the load that the film can withstand is reduced because the attraction between layers is reduced. A benchmark for the wet-state mechanical properties of these films containing oppositely charged

polyelectrolytes were reported previously (Nolte et al. 2009), with a modulus between 140 to 750 MPa dependent upon the composition of the film (Moehwald et al. 2003).

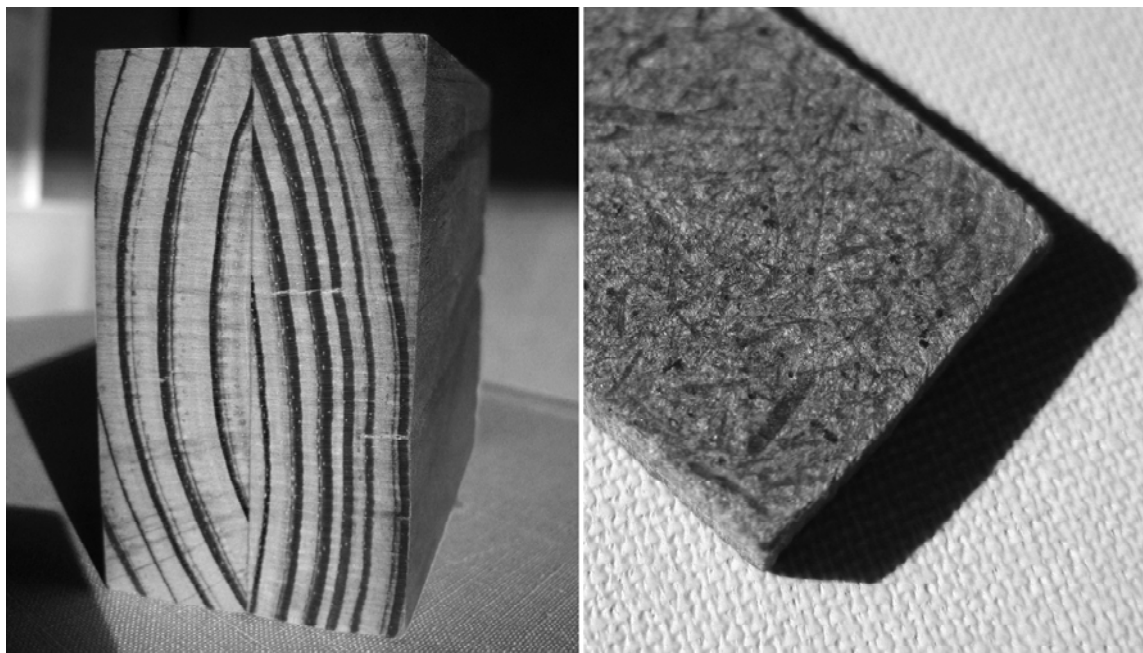


Fig. 1. (Left) Wood blocks that are 18mm thick bonded together with polyelectrolyte multilayer films. (Right) 12 mm wide compression molded fiber-based composites containing fibers treated with polyelectrolytes prior to consolidation.

Crosslinking of Films and Water Resistant Bonds

Polyelectrolytes containing amino/ammonium and acid/carboxylate functionality can be crosslinked to form covalent bonds to reduce their susceptibility of the intermolecular forces to the medium (Schuetz and Caruso 2003). The crosslinking can be detected using FTIR by the absorbance of amide peaks ($\nu=1671\text{ cm}^{-1}$ (NC=O)) after crosslinking at temperatures between 130 and 250°C (Harris et al. 1999). Transmission FTIR spectroscopy of films that were 15 bi-layers thick, on silicon substrates, were studied as a function of temperature, heated for two hours (Fig. 2). A nylon-like amide absorbance peak at $\nu=1671\text{ cm}^{-1}$ (NC=O) was evident in the spectra, while the amide bond II at $\nu=1540\text{ cm}^{-1}$ was masked by other peaks (Harris et al. 1999). As temperature increased, the normalized absorption of amide stretch at $\nu=1671\text{ cm}^{-1}$ increased linearly for temperatures ranging from 150 to 250°C. This change suggests that crosslink density between the polyelectrolyte films increased with temperature. Heating for less than two hours resulted in no clear amide formation in the spectra at 1671 cm^{-1} , as peak positions within the shorter time periods overlap the control data shown in Fig. 2. It should be noted that the region where the amide absorption occurs have overlapping peaks that would cause any small changes within the film to show up as broadening of a shoulder. Hence, low levels of crosslinking would provide minimal change to the spectra.

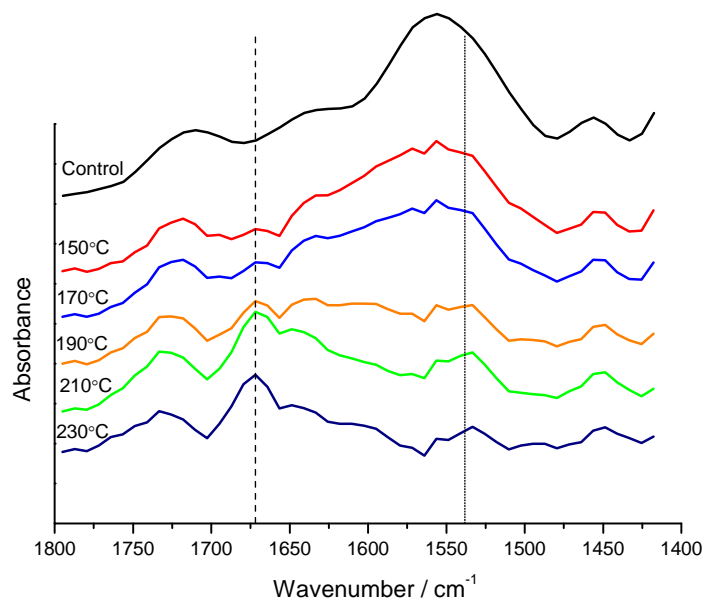


Fig. 2. FTIR spectra of 15 bi-layer PEI(PAA/PAH) films heated to varying temperatures for 120 minutes. Note appearance of peak at $\nu=1671\text{ cm}^{-1}$ related to amide bond formation.

Wooden substrates coated with the LbL films of varying bi-layer number were allowed to dry in a conditioning chamber. These materials were then sprayed with water at their surface, placed in contact, and subsequently heated. As noted by Matsukuma et al. (2009) the water allows for polymer mobility and intimate contact between polyelectrolyte layers. Specimens with bondline temperatures elevated above 150°C remained adhered upon exposure to liquid water, and even under severe repeated exposure of 4h in boiling water. The attained water-resistant property of the bondline conflicted with the FTIR results, in which the amide bond of the model films was not clearly detected for 30 minute time periods. Eriksson and co-workers found evidence of crosslinking within PAH/PAA films formed on pulp fibers after heating to 160°C for 30 minutes (Eriksson et al. 2006). In that study, no clear amide peak at 1671 cm^{-1} was reported; instead an increase in the area for 1540 cm^{-1} was used to establish crosslinking.

Additional FTIR analysis of PEI on wood did not reveal specific changes related to PEI on wood. Changes in absorbance between $1700\text{--}1600\text{ cm}^{-1}$ were overshadowed by the response of wood because of the thermal treatment (data not shown). Moreover, PEI has been shown to bond wood when heated above 120°C , with the bondline able to withstand exposure to water (Liu and Li 2006b). Because PEI has a number of primary, secondary, and tertiary amines, it is possible that sufficient hydrogen bonding can occur with the wood cell wall components even if there are no chemical reactions with available functional groups of wood (Liu and Li 2006a). Hence, the PEI as the primary interacting layer may help add to the LbL bondline stability through secondary interactions.

The relationship between the number of layers and relative bonding strength was investigated using a compression shear block test. As a control, commercial phenol formaldehyde (PF) resin was also investigated. The shear strength of multilayer bonded specimens increased as a function of the number of layers (Fig. 3). A corresponding increase in the failure of the substrate surface also occurred with multilayers of 6, 10, and 18 bi-layers having an average percentage of wood surface failure of 5%, 19%, and 73%, respectively. An example of a failed LbL surface is provided in Fig. 3. PF adhesive had an average of 47% failure, and all samples tested wet showed zero failure of the wood surface. Shear strengths were reduced for all specimens tested wet, after the weathering experiments, revealing a similar trend between shear strength and the number of bi-layers (Fig. 3).

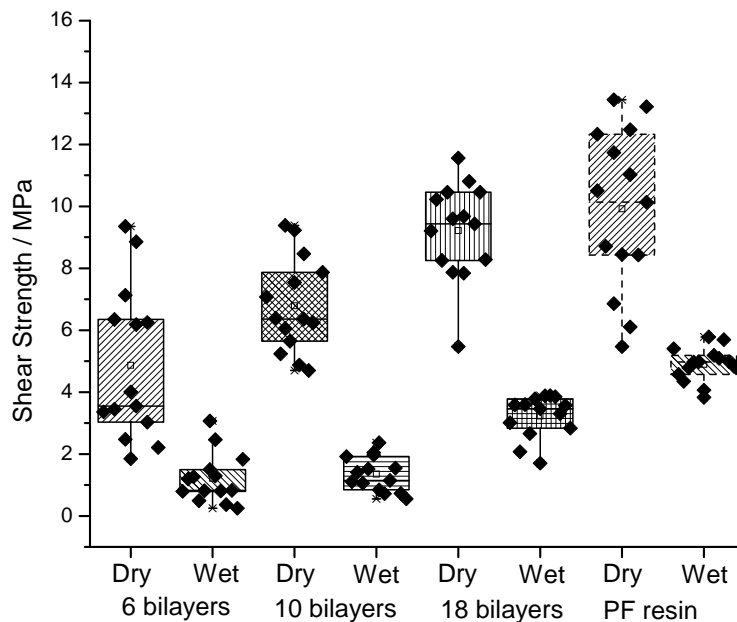


Fig. 3. Compression shear strength of wood blocks treated with LbL films as a function of total number of bi-layers in the bondline. Wet samples underwent two 4-hour boil cycles and then were tested wet at room temperature.

A difference in surface structure on the wood was evident when comparing 3 and 9 bi-layers of coating. As shown, the fine structure of the wood surface became partially masked by the 9 bi-layer films (Fig. 4). The wood surface with 3 bi-layers contained features such as jagged fractured wall layers. In contrast, substrates with 9 bi-layers appeared coated with texture across the wood surface (Fig. 4). A thicker coating would allow greater interdiffusion of the polyelectrolyte chains at the interface when two blocks are placed in contact. Hence, a greater number of bi-layers may serve to ensure bridging of the films between samples. Polymer entanglements between multilayer films have been implicated in developing adhesion strength between multilayer films, with an increase in layer number facilitating polymer interdiffusion (Johansson et al. 2009). Furthermore, Eriksson and co-workers found joint strength and tensile index of paper handsheets increased with the number of layers deposited on the fiber (Eriksson et al. 2006). Although not addressed in this current study, compliance of the substrate and applied pressure are also variables that impact the degree of contact between substrates and may influence the mechanical properties.

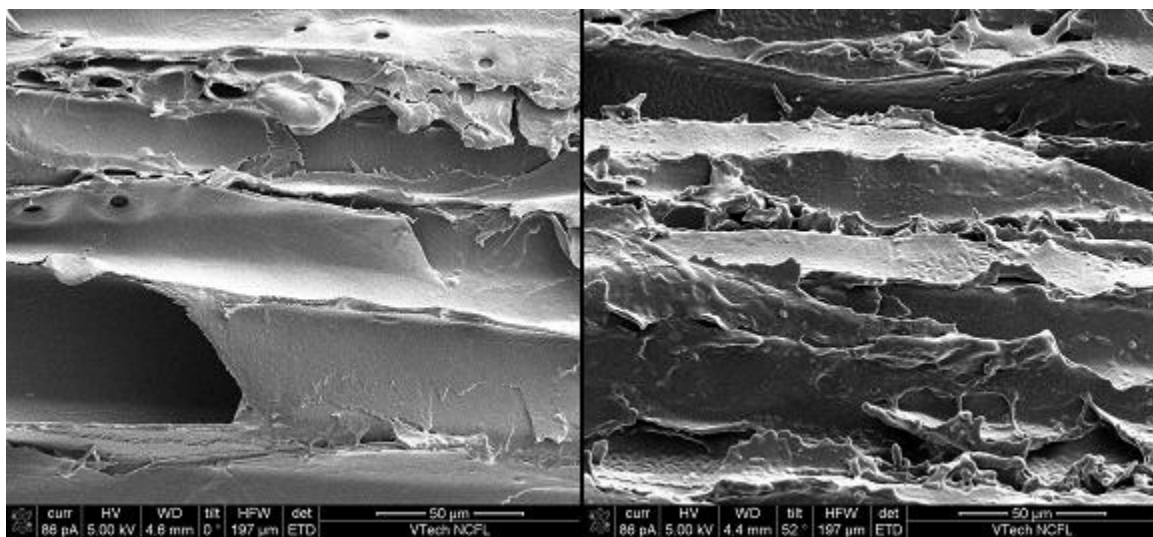


Fig. 4. The cut surface of wood parallel to the stem axis modified with polyelectrolyte multilayers, (left) 3 bi-layers and (right) 9 bi-layers. Wood surfaces have micron scale roughness due to the tracheid cell elements which are ~50 micrometers in diameter and 3 to 5 millimeters in length.

Equivalency between mechanical properties from compression shear block tests and engineering values for composite material performance are not direct. Therefore, pressure refined wood fibers were coated with 3 and 3.5 bi-layers and subsequently compression molded into plaques ($\rho=1150 \text{ kg/m}^3$) at 180°C .

Fiber surfaces prior to consolidation had a similar appearance for both uncoated and 3.5 bi-layer coated fibers (Fig. 5). No clear evidence of the coating is seen in the Fig. 5b. This finding of the visible fiber structure beneath the nanoscale coating is similar to what is seen in Fig. 4 for the 3 bi-layer coated samples on the wood surfaces.

The flexural modulus (MOE) of the samples was 6.78 GPa (COV 8%) and the modulus of rupture (MOR) was 107 MPa (COV 6%). These values were remarkably higher than comparative reference values (Youngquist 1999). Values were up to two

times larger than other fiber composites, and the fibers were not oriented for the testing direction as commonly found for panel products. In fact, these values begin to approach structural based panels used in applications such as wall and roof sheathing (Youngquist 1999). However in this case, the bondlines were a maximum of 75 nm thick at an estimated level of 3% by weight. As a control, untreated fibers were pressed using similar conditions and the average values were 2.09 GPa and 16.35 MPa for MOE and MOR, respectively.

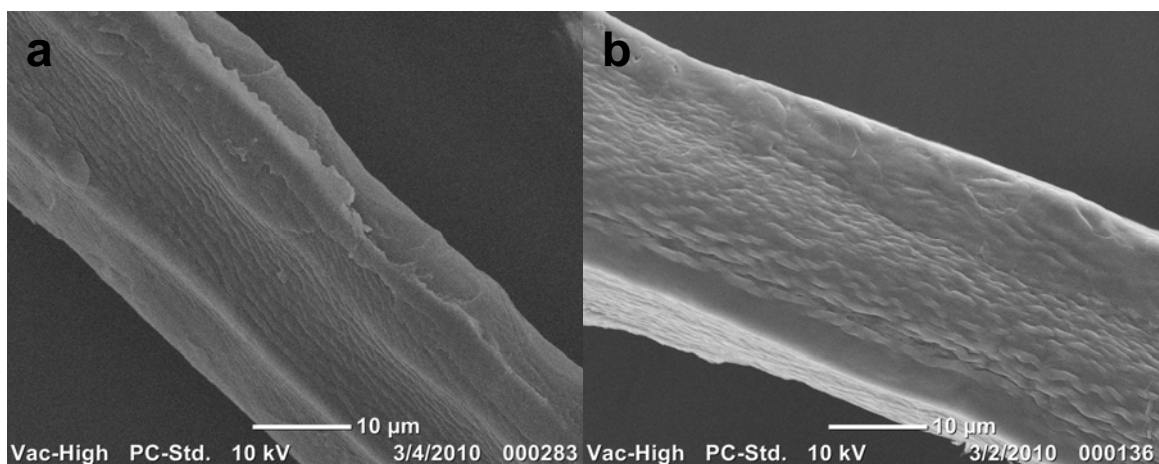


Fig. 5. a) Unmodified pressure refined fiber and b) fiber modified with 3.5 bi-layers of polyelectrolytes. Note, the lack of clear indication of a coating on the fiber surfaces.

Based on the ability to form LbL films on many different materials, simple substitution of glass fibers with LbL films on their surfaces may be used to create hybrid fiber composite materials that have adequate adhesion across inorganic and organic phases. Additionally, other materials like clay platelets (Lin et al. 2008), enzymes (Xing et al. 2007), TiO₂ (Lu et al. 2007), metal nanoparticles (Dong and Hinestroza 2009), and conductive polymers (Agarwal et al. 2006) have been incorporated onto the surfaces of natural fibers, creating facile routes to tailor fiber-based materials. The enhancement of properties of plant biomass with layer-by-layer films may provide sustainable materials for more advanced applications when considering recent work on ultra-strong materials of crosslinked nanoparticle reinforced films (Shim et al. 2009). With the versatility of film formation on virtually any surface, LbL films offer a route to adhere dissimilar materials together with stable bondline chemistries. As nanoscale properties are difficult to manufacture into macroscale materials, scale-integrated approaches are sought; this study demonstrated that LbL films with nanoscale architecture offer a unique route for substrate adhesion.

CONCLUSIONS

1. Wood surfaces that are chemically heterogeneous with inherent roughness were adhered together with LbL films, providing for adhesive bondlines with adhesive strength

similar to that of commercial adhesive technologies. Increasing the number of bi-layers deposited on the wood surfaces increased the resulting shear strength of the specimens.

2. Crosslinking of the PAH/PAA films was evident on silicon surfaces for extended heating times for temperatures above 150°C. The development of cross-linking peaks on the films was not correlated with the dimensional stability of the bonded wood specimens. The bonded wood specimens were water-resistant after heating the samples for 30 minutes, although at this time period of heating model films no clear cross-linking peak was observed in the spectra.

3. Wood fiber-based composites were created with LbL adhesives that had stiffness similar to strand-based structural composites.

ACKNOWLEDGMENTS

This project was supported by the Wood-based Composites Center; the USDA CSREES, Special Research Grant No. 2008 - 34489 – 19377; the Sustainable Engineered Materials Institute, Virginia Tech; and the Institute for Critical Technology and Applied Science, Virginia Tech, Blacksburg, Virginia.

REFERENCES CITED

- Agarwal, M., Lvov, Y., and Varahramyan, K. (2006). "Conductive wood microfibrils for smart paper through layer-by-layer nanocoating," *Nanotechnology* 17(21), 5319-5325.
- Baer, E., Hiltner, A., and Morgan, R. J. (1992). "Biological and synthetic hierarchical composites," *Phys. Today* 45(10), 60-7.
- Cebeci, F. C., Wu, Z., Zhai, L., Cohen, R. E., and Rubner, M. F. (2006). "Nanoporosity-driven superhydrophilicity: A means to create multifunctional antifogging coatings," *Langmuir* 22(6), 2856-2862.
- Choi, J. and Rubner, M. F. (2005). "Influence of the degree of ionization on weak polyelectrolyte multilayer assembly," *Macromolecules* 38(1), 116-124.
- Decher, G. (1997). "Fuzzy nanoassemblies: Toward layered polymeric multicomposites," *Science* 277(5330), 1232-1237.
- Dong, B. H. and Hinstroza, J. P. (2009). "Metal nanoparticles on natural cellulose fibers: Electrostatic assembly and in situ synthesis," *ACS Appl. Mater. Interfaces* 1(4), 797-803.
- Eriksson, M., Torgnysdotter, A., and Wågberg, L. (2006). "Surface modification of wood fibers using the polyelectrolyte multilayer technique: Effects on fiber joint and paper strength properties," *Ind. Eng. Chem. Res.* 45(15), 5279-5286.
- Han, J. T., Zheng, Y., Cho, J. H., Xu, X., and Cho, K. (2005). "Stable superhydrophobic organic-inorganic hybrid films by electrostatic self-assembly," *J. Phys. Chem. B* 109(44), 20773-20778.

- Harris, J. J., DeRose, P. M., and Bruening, M. L. (1999). "Synthesis of passivating, nylon-like coatings through crosslinking of ultrathin polyelectrolyte films," *J. Am. Chem. Soc.* 121(9), 1978-1979.
- Israelachvili, J. (1991). *Intermolecular and Surface Forces*, (ed.), Academic Press, Amsterdam.
- Izquierdo, A., Ono, S. S., Voegel, J. C., Schaaf P., and Decher, G. (2005). "Dipping versus spraying: Exploring the deposition conditions for speeding up layer-by-layer assembly," *Langmuir* 21(16), 7558-7567.
- Johansson, E., Blomberg, E., Lingstrom, R., and Wågberg, L. (2009). "Adhesive interaction between polyelectrolyte multilayers of polyallylamine hydrochloride and polyacrylic acid studied using atomic force microscopy and surface force apparatus," *Langmuir* 25(5), 2887-2894.
- Kachurina, O., Knobbe, E., Metroke, T. L., Ostrander, J. W., and Kotov, N. A. (2004). "Corrosion protection with synergistic LBL/ormosil nano-structured thin films," *Int. J. Nanotechnol.* 1(3), 347-365.
- Kolasinska, M., Krastev, R., and Warszynski, P. (2007). "Characteristics of polyelectrolyte multilayers: Effect of PEI anchoring layer and post-treatment after deposition," *J. Colloid Interf. Sci.* 305(1), 46-56.
- Krogman, K. C., Zacharia, N. S., Schroeder, S., and Hammond, P. T. (2007). "Automated process for improved uniformity and versatility of layer-by-layer deposition," *Langmuir* 23(6), 3137-3141.
- Lee, H., Lee, Y., Statz, A. R., Rho, J., Park, T. G., and Messersmith, P. B. (2008). "Substrate-independent layer-by-layer assembly by using mussel-adhesive-inspired polymers," *Adv. Mater. (Weinheim, Ger.)* 20(9), 1619-1623.
- Li, Y., Liu, F., and Sun, J. (2009). "A facile layer-by-layer deposition process for the fabrication of highly transparent superhydrophobic coatings," *Chem. Commun. (Cambridge, U. K.)* 19, 2730-2732.
- Lin, Z., Renneckar, S., and Hindman, D. P. (2008). "Nanocomposite-based lignocellulosic fibers 1. Thermal stability of modified fibers with clay-polyelectrolyte multilayers," *Cellulose* 15(2), 333-346.
- Lingstrom, R., Wågberg, L., and Larsson, P. T. (2006). "Formation of polyelectrolyte multilayers on fibres: Influence on wettability and fibre/fibre interaction," *J. Colloid Interf. Sci.* 296(2), 396-408.
- Liu, Y. and Li, K. (2006a). "Development and characterization of adhesives from soy protein for bonding wood," *Int. J. Adhes. Adhes.* 27(1), 59-67.
- Liu, Y. and Li, K. (2006b). "Preparation and characterization of demethylated lignin-polyethylenimine adhesives," *J. Adhes.* 82(6), 593-605.
- Lu, Z., Eadula, S., Zheng, Z., Xu, K., Grozdits, G., and Lvov, Y. (2007). "Layer-by-layer nanoparticle coatings on lignocellulose wood microfibers," *Colloid Surface A* 292(1), 56-62.
- Lvov, Y. M., Grozdits, G. A., Eadula, S., Zheng, Z., and Lu, Z. (2006). "Layer-by-layer nanocoating of mill broken fibers for improved paper," *Nord. Pulp Pap. Res. J.* 21(5), 552-557.

- Matsukuma, D., Aoyagi, T., and Serizawa, T. (2009). "Adhesion of two physically contacting planar substrates coated with layer-by-layer assembled films," *Langmuir* 25(17), 9824-9830.
- Moehwald, H., Donath, E., and Sukhorukov, G. (2003). "Smart capsules," *Multilayer Thin Films* 363-392.
- Nolte, A. J., Chung, J. Y., Walker, M. L., and Stafford, C. M. (2009). "In situ adhesion measurements utilizing layer-by-layer functionalized surfaces," *ACS Appl. Mater. Interfaces* 1(2), 373-380.
- Notley, S. M., Eriksson, M., and Wågberg, L. (2005). "Visco-elastic and adhesive properties of adsorbed polyelectrolyte multilayers determined in situ with QCM-D and AFM measurements," *J. Colloid Interf. Sci.* 292(1), 29-37.
- Rennekar, S. and Zhou, Y. (2009). "Nanoscale coatings on wood: Polyelectrolyte adsorption and layer-by-layer assembled film formation," *ACS Appl. Mater. Interfaces* 1(3), 559-566.
- Schlenoff, J. B., Dubas, S. T., and Farhat, T. (2000). "Sprayed polyelectrolyte multilayers," *Langmuir* 16(26), 9968-9969.
- Schuetz, P. and Caruso, F. (2003). "Copper-assisted weak polyelectrolyte multilayer formation on microspheres and subsequent film crosslinking," *Adv. Funct. Mater.* 13(12), 929-937.
- Shchukin, D. G., Zheludkevich, M., Yasakau, K., Lamaka, S., Ferreira, M. G. S., and Moehwald, H. (2006). "Layer-by-layer assembled nanocontainers for self-healing corrosion protection," *Adv. Mater. (Weinheim, Ger.)* 18(13), 1672-1678.
- Shim, B. S., Zhu, J., Jan, E., Critchley, K., Ho, S., Podsiadlo, P., Sun, K., and Kotov, N. A. (2009). "Multiparameter structural optimization of single-walled carbon nanotube composites: toward record strength, stiffness, and toughness," *ACS Nano* 3(7), 1711-1722.
- Wågberg, L., Forsberg, S., Johansson, A., and Juntti, P. (2002). "Engineering of fibre surface properties by application of the polyelectrolyte multilayer concept. Part I: Modification of paper strength," *J. Pulp Pap. Sci.* 28(7), 222-228.
- Wang, R. Z., Suo, Z., Evans, A. G., Yao, N., and Aksay, I. A. (2001). "Deformation mechanisms in nacre," *J. Mater. Res.* 16(9), 2485-2493.
- Xing, Q., Eadula, S. R., and Lvov, Y. M. (2007). "Cellulose fiber-enzyme composites fabricated through layer-by-layer nanoassembly," *Biomacromolecules* 8(6), 1987-1991.

Article submitted: October 12, 2009; Peer review completed: Jan. 17, 2010; Revised version received and accepted: June 1, 2010; Published: June 2, 2010.